Electronic Supplementary Material (ESI) for Nanoscale Advances.
This journal is © The Royal Society of Chemistry 2023

**Electronic Supplementary Information (ESI)**

# Interfacial negative magnetization in Ni encapsulated layer tunable nested $MoS_2$ nanostructure for robust memory applications

*Shatabda Bhattacharya[1,2], Tatsuhiko Ohto[2], Hirokazu Tada[2] and Shyamal K. Saha[1*]*

[1]School of Materials Sciences, Indian Association for the Cultivation of Science, Jadavpur, Kolkata-700032, India

[2]Department of Materials Engineering Science, Graduate School of Engineering Science, Osaka University, Toyonaka, 560-8531, Japan

e-mail address of the corresponding author: cnssks@iacs.res.in

## A. Additional Characterizations

### A1. Magnified HR-TEM images of the hybrid structures :

In the additional magnified portions of TEM images (from Fig. 1), the in-plane Ni crystalline phases can be seen along with $MoS_2$ interlayers as shown below. For better clarity, the Ni regions are marked with yellow circles. (**Fig. S1 (a), (b)**) It was observed that for thin $MoS_2$ layers, the Ni phase can seen very sharply (In Fig .1f main manuscript).

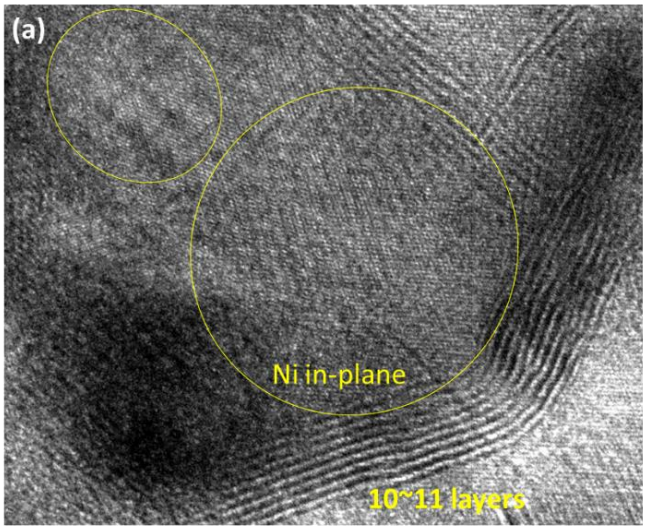


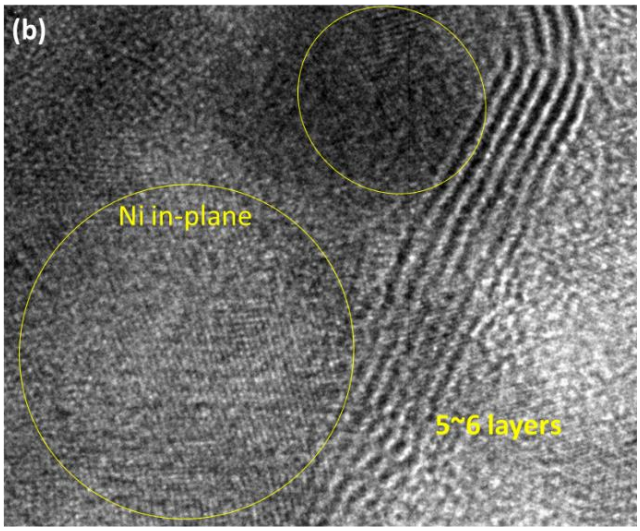


(b)

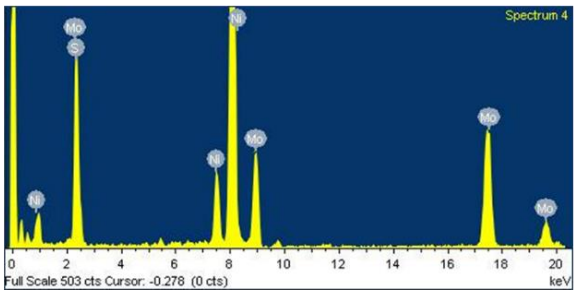


| Element | Peak | Area | k | Abs | Weight% | Weight% | Atomic% |
|---|---|---|---|---|---|---|---|
| | Area | Sigma | factor | Corrn. | | Sigma | |
| S K | 2490 | 209 | 0.940 | 1.000 | 39.93 | 1.28 | 64.49 |
| Ni K | 1204 | 71 | 1.245 | 1.000 | 10.64 | 0.64 | 3.74 |
| Mo K | 1339 | 121 | 2.996 | 1.000 | 49.43 | 2.32 | 31.77 |
| Totals | | | | | 100.00 | | |

***Fig. S1*** *(a): Magnified TEM image of 10-11 layares of $MoS_2$ with inplane Ni-nanophase. The crystalline phases of Ni is highlighted inside the circles. (b) For 5~6 layers of $MoS_2$ with inplane Ni-nanophase. (C) EDAX mapping during TEM analysis shows the elements detetced along with the table for atomic and weight percentages.*

**A2: Energy Dispersive Absorption X-Ray Analysis (EDAX):** For elemental identification and presence of impurities we have perfomed EDAX analysis of a typical M2 sample during TEM experiment. The insitu analysis was conducted for 48s exposure in an accelerating potential of 200.00 kV. As seen from the EDAX profile, other than Mo, S and Ni peaks, no presence of trace O peak was detetected. The atomic % of Mo:S is neraly 2 which verifies the composition of phase with good stiotiometric ratio.

**A3. Avergae layer number analysis from TEM images:** To quantify the average layer number in $MoS_2$, we measured from different nanoparticle images and from there found that for thick $MoS_2$ layers (M1) have 9-14 number of layers with the histogram centered around 11. For M2 the layer numbers vary from 3-6 with the standard distribution centered around 5 and for M3, it varies between 1-4 number of layers, with the average being 2 layers.

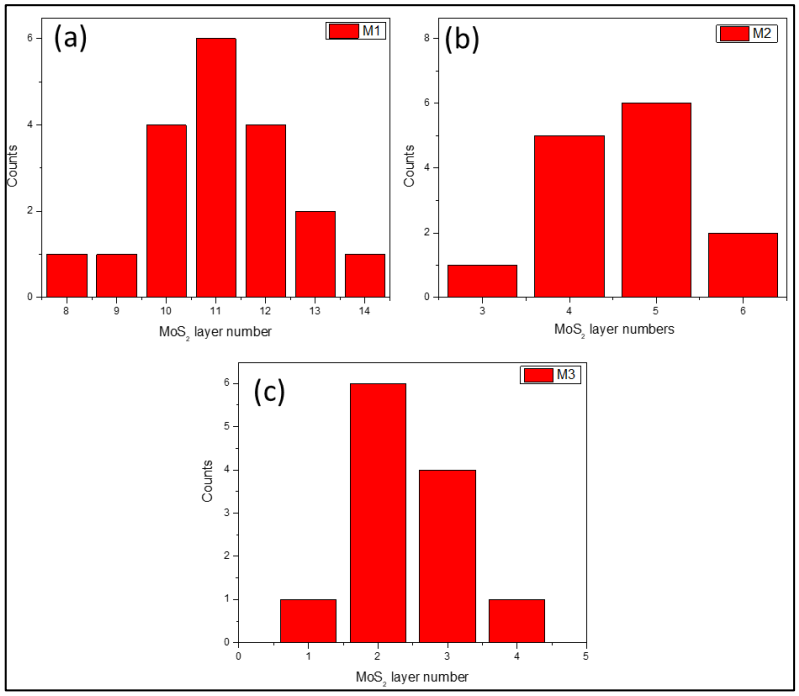


***Fig.S2****: (a), (b) and (c) Layer number histogram plot for M1. M2 and M3 respectively.*

**B. ZFC-FC plot of spontaneous magnetization:**

At room temperature if dc positive field is applied (FC protocol) the magnetization automatically switches to positive side. In **Fig. S3(a)**, we have shown the ZFC-FC curves for 50 Oe magnetic field in the same plot in which a ferromagnetic saturation is observed at lower temperature in FC process. The bifurcation between FC and ZFC process continues up-to room temperature 300K indicating the ferromagnetic exchange ordering at elevated temperatures.

The ZFC measurement under negative dc field as shown in **Fig. S3(b)** and plotted with the positive field of ZFC (+50 Oe) to ascertain the direction of magnetization in the two cases. Interestingly, it is found that in the low temperature region, a complete mirror reflection of +50 Oe ZFC has been obtained for -50 Oe ZFC process. It means, during -50 Oe cooling, the direction of the magnetization of the sample becomes positive. Therefore, confirming the negative magnetization state in the present sample is not due to the trap field of the superconducting magnet in the SQUID magnetometer.

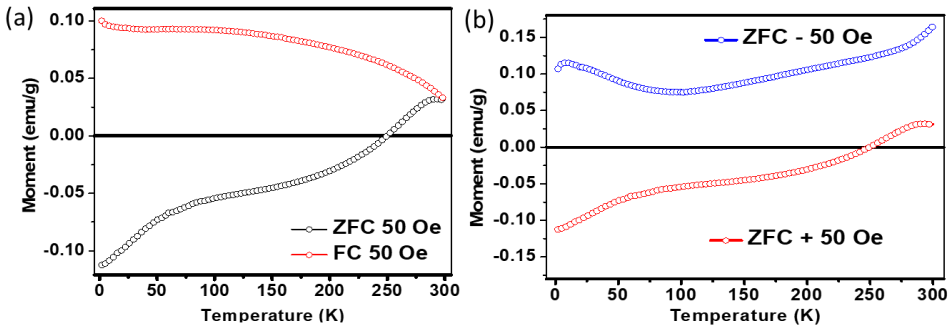


***Fig. S3:*** *(a) ZFC-FC curves for a typical sample show the bifurcation up-to temperature 300K. (b) Moment vs. temperature ZFC curve at positive and negative magnetic fields.*

**C. Explanation of spin orientation at the interface at different temperatures**

At room temperature 300K, spin distribution in the absence of magnetic field within the Ni and $MoS_2$ was initially like in **Fig. 3(d)** [In main manuscript]. Here yellow spins refer to the Ni and red color spins represent the spins generated because of charge transfer in the $MoS_2$ layers. With decreasing temperature magnetic moment of Ni at the interface slowly increases compared to the moment of '$MoS_2$' spin due to charge transfer effect as the amount of charge transfer increases with decreasing temperature. At an intermediate temperature the magnitude of Ni spin and $MoS_2$ spin become equal and

opposite. Hence net magnetization is zero at this temperature. This may be called compensate temperature ($T_c$) where net magnetization will be zero due to perfect antiparallel arrangement. If we reduce the temperature further, charge transfer rate again increases and magnitude of $MoS_2$ spin moment will be greater than Ni spin moment at the interface. Because of the Ni spins are in random orientation at the core of the Ni particle, the net magnetization is dominated by the spins generated in the $MoS_2$ layer due to charge transfer effect. Therefore, at the lowest measured temperature, under ZFC process, magnetization shows negative value because of larger spin moment of '$MoS_2$' compared to that of Ni phase and the effective net magnetization will be in the direction of $MoS_2$ spin.

**D. Anomalous enhancement of coercivity and giant exchange bias with temperature**

To find the strength of exchange field, we already calculated average coercivity for all the samples at particular temperatures using the formula $H_C = \left(\left|H_C^+\right| + \left|H_C^-\right|\right)/2$ where $H_c^+$ and $H_c^-$ are the positive and negative coercive fields respectively**.** However, because of this asymmetry in coercive fields, the strength of FC exchange bias is calculated from FC MH loops $H_E = \left(H_C^+ + H_C^-\right)/2$ **Table SI** shows the variation of FC exchange bias with temperature for all the samples. The sample is cooled from 300K to 2K in presence of magnetic field of 1000 Oe and then measured the M-H loops at different temperatures. The interesting part is that a huge shift of coercive field is obtained as shown in **Fig. S4**. Therefore, from this large shift in coercive field it is confirmed that both ferromagnetic and antiferromagnetic coupling is very strong here.

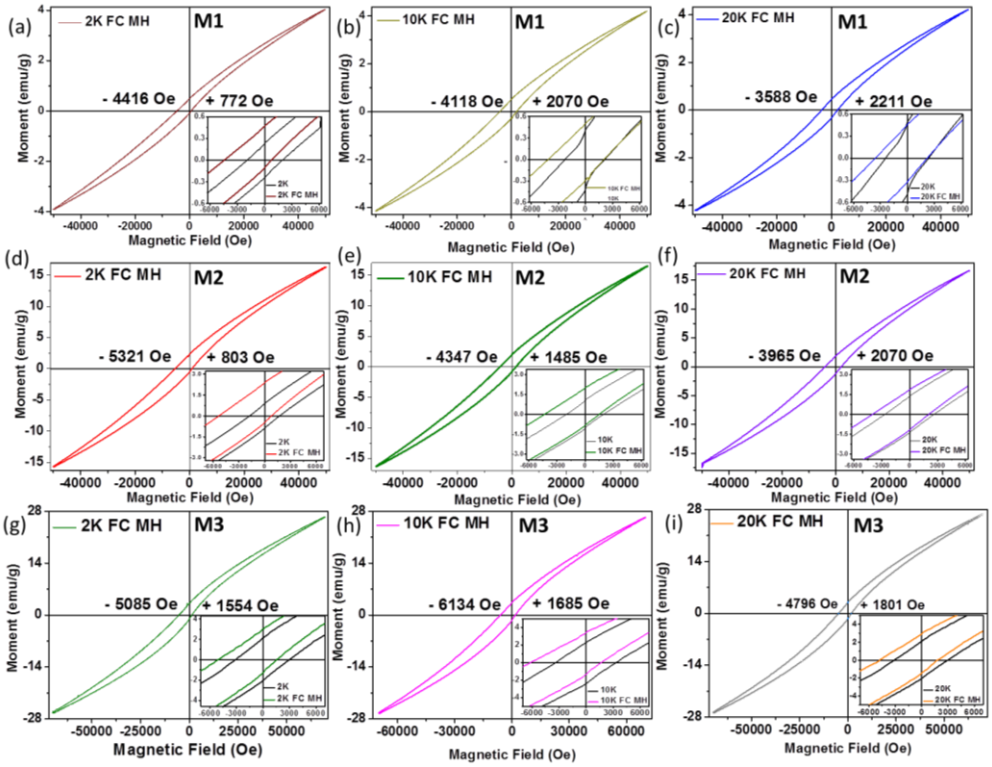

***Fig. S4****. Field cooled MH loop showing the high amount of asymmetry due to giant exchange bias. (a)-(c) for sample M1, (d)-(f) for M2 and (g)-(i) for M3 at temperatures 2K, 10K and 20K respectively.*

**Table SI: Variation of FC exchange bias with temperature**

| M1 | | | | M2 | | | | M3 | | | |
|---|---|---|---|---|---|---|---|---|---|---|---|
| T(K) | $H_c^+$ | $H_c^-$ | FC Exchange Bias (Oe) | T(K) | $H_c^+$ | $H_c^-$ | FC Exchange Bias (Oe) | T(K) | $H_c^+$ | $H_c^-$ | FC Exchange Bias (Oe) |
| 2 | 772 | -4416 | -1822 | 2 | 803 | -5321 | -2259 | 2 | 1554 | -5085 | -1765 |
| 10 | 2070 | -4118 | -1024 | 10 | 1485 | -4347 | -1431 | 10 | 1685 | -6134 | -2224 |
| 20 | 2211 | -3588 | -688 | 20 | 2070 | -3965 | -947 | 20 | 1801 | -4796 | -1497 |

**E. Additional magnetic characterization plots (**Plot of coercivity vs. temperature and ZFC exchange bias vs. temperature; Initial magnetization grow vs. applied field; high temperature MH loops for all the samples. Fig. caption is in below**)**

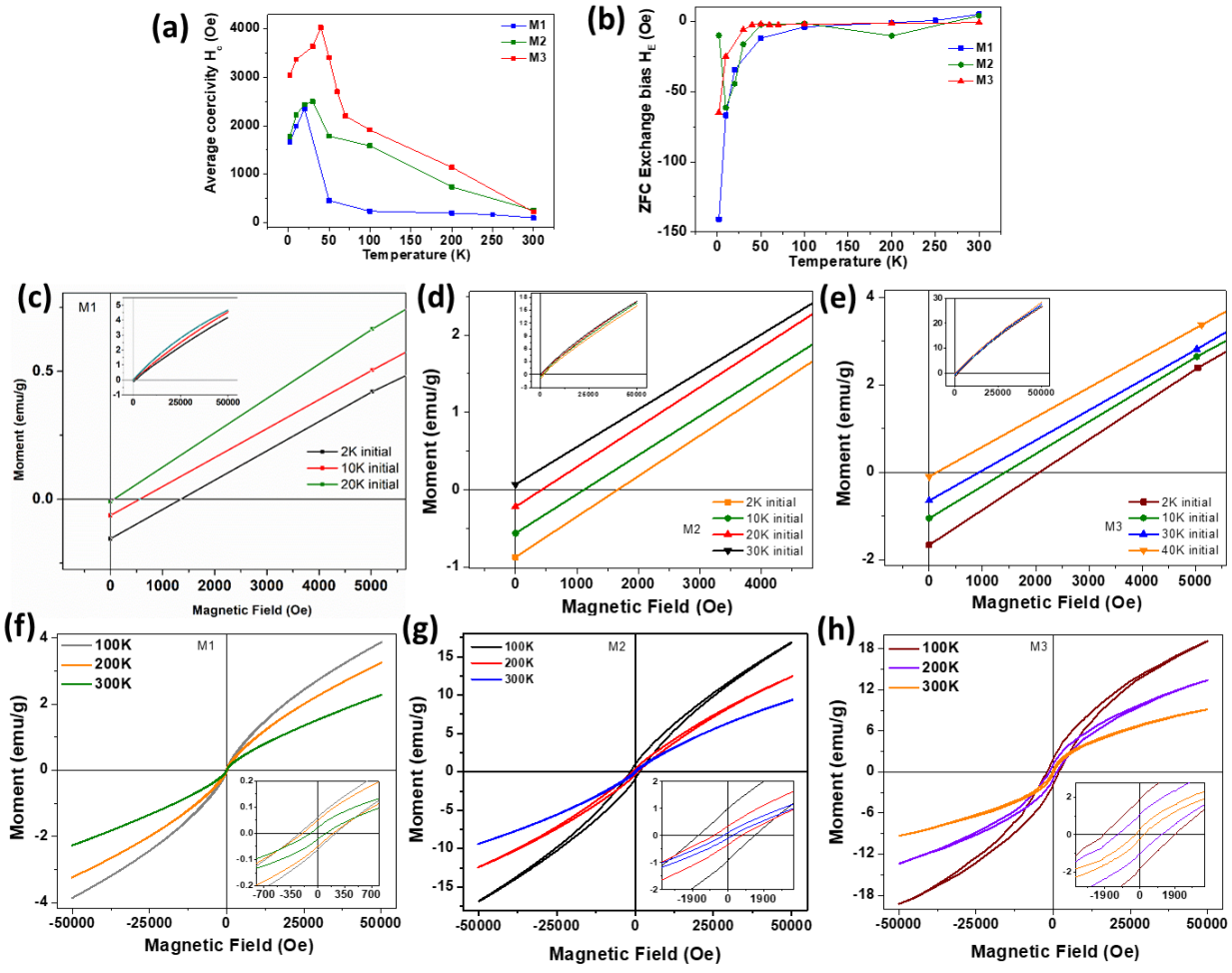

***Fig. S5****. (a) variation of average coercivity with temperature (b) variation of ZFC exchange bias with temperature (c-e): Initial growth of negative magnetization with applied field during MH loop for M1, M2 and M3 respectively. The magnified version shows negative magnetization at zero field which was also observed during ZFC study. The inset graph is full view. (f-h): High temperature MH loop for M1, M2 and M3 respectively with insets magnified view near zero field region.*

**F. Schematic for anomalous increment of magnetic parameters with temperature**

We have considered the schematic diagram as shown in **Fig. S6** to understand the anomalous increase of magnetic parameters with temperature. At the lowest temperature 2K, spins are randomly frozen within the soft Ni core phase with AFM coupling at the interface (**Fig. S6(a)**). When isothermal magnetization vs. field has started, with increasing field the soft-core spins start to rotate in the field direction (**Fig. S6(b))**. When the system temperature is increased, the charge transfer across the interface is reduced and as a result, '$MoS_2$' spin moment decreases rapidly compared to 'Ni' spin moment resulting net enhancement of magnetization with increase in temperature. In other words, ferromagnetic interaction increases at the expense of antiferromagnetic interaction (**Fig. S6(c))** resulting enhancement in both the coercivity and magnetic moment. If the temperature is increased further, the $MoS_2$ spins are merged within the domain of Ni core and total number of spins contributing magnetization increase. So, specific magnetic moment rises with temperature (**Fig. S6(d)**).

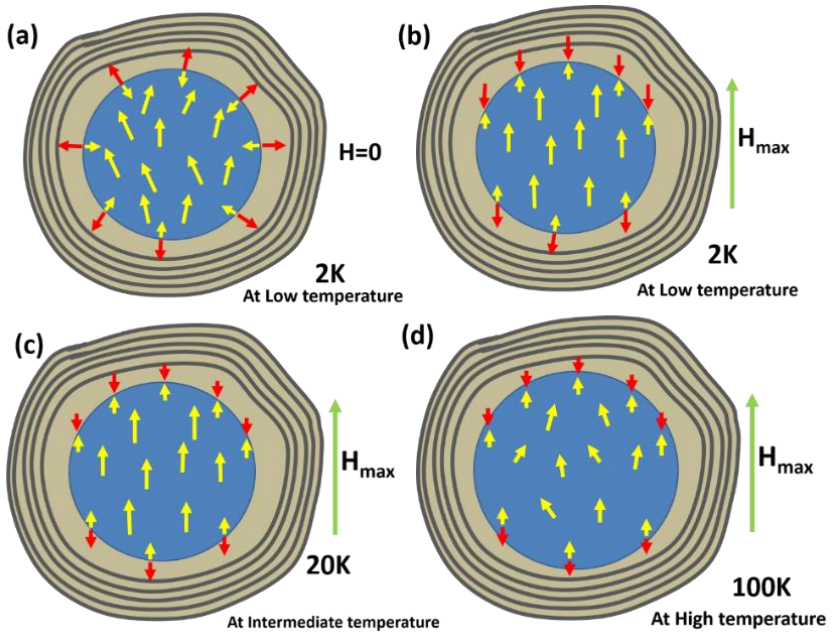

***Fig. S6****. Schematic model for the anomalous increasing of coercivity and magnetization with temperature. Spin distributions at the interface (a) at 2K with zero field (b) at 2K with applied field (c) at 20K and (d) at 100K.*

**G. Measurement protocol for long relaxation in ZFC-FC techniques:**

During ZFC process, the sample is initially cooled under constant cooling rate of 3K/min to a temperature $T_0$=100K. After reaching $T_0$, a 50 Oe field is applied and magnetization is recorded as a function of time $t_1$ for 2000 Sec. After time $t_1$, the sample is quickly quenched to a lower temperature 90K ($T_0$-ΔT) and magnetization is recorded for period of time $t_2$ (2000 Sec). Ultimately, the temperature is quickly swept back to $T_0$ and magnetization is recorder for another period of time $t_3$ (2000 Sec). Magnetization is plotted as a function of continuous measurement time t. For quick changing the temperature from $T_0$, we used very fast thermal ramping rate (8K/min) in the SQUID VSM (Quantum Design) machine.

**H. Role of Ageing effect and wait time dependence on magnetization memory state**

$$M(t) = M_0 - M_r \exp\left[-\left(\frac{t}{\tau}\right)^{\beta}\right] \quad \text{.....(1)}$$

In this equation $M_r$, τ (characteristics relaxation time) and β (stretching parameter) are proportionate function of temperature and wait time $t_w$ respectively. Actually, the value of β relies on the nature of energy barriers that are involved in the relaxation process. It is seen that the value of the time constant τ increases with the increasing wait time $t_w$ which implies the stiffening of spin relaxation i.e. ageing effect with increasing wait time before measurement. One can increase the memory effect at a particular temperature by applying a wait time before measurement which can retain the magnetization state for a longer time due to ageing effect. It is also found that β increases with wait time i.e. energy barrier is increased with wait time. Then more energy is required to destroy the memory effect. It also defines temperature stabilization on magnetization relaxation. This is due to the fact that application of greater wait time before measurement creates a thermal stabilization in the system. The more the wait time, stronger is the interaction among the magnetic clusters. Therefore, due to greater interaction β value is also increased with increasing wait time.

**I. Thermo remnant magnetization (TRM) measurement protocol for wait time dependence**

It should be noted that this equation should be applied to understand the relaxation rate for the decay of thermo remnant magnetization (TRM) and not for the ordinary ZFC magnetization as studied earlier. In

this study the TRM is measured in the following procedure: First the sample is magnetized by applying a magnetic field at 300K. Then it is cooled from 300K at cooling rate of 4K/min in the presence of 50 Oe dc magnetic field to the desired measuring temperatures. After reaching the desired measuring temperature a wait time of 5000 Seconds was given. Then the magnetic field is switched off and time decay of magnetization is recoded.

**Table SII: Parameters obtained after fitting with Eq. (6) in Fig. 9 (temp variation and field variation)**

| **Temp Variation** | n | | A | |
|---|---|---|---|---|
| | Value | Error | Value | Error |
| 1.8K | 0.79 | 0.0165 | 0.0011 | 6.648E-5 |
| 10K | 0.88 | 0.0041 | 0.0053 | 1.240E-4 |
| 100K | 0.94 | 0.0013 | 0.0034 | 2.556E-4 |
| **Field Variation** | n | | A | |
| | Value | Error | Value | Error |
| 50 Oe | 0.85 | 0.0017 | 0.0249 | 2.1011E-4 |
| 100 Oe | 0.90 | 0.0024 | 0.0212 | 1.82296E-4 |
| 200 Oe | 0.93 | 0.0015 | 0.0201 | 1.40293E-4 |